ORIGINAL PAPER

Antibacterial, DNA photocleavage and molecular docking studies of newly prepared Schiff-based macrocyclic complexes

Purti Mishra [1], Pooja Sethi [1], Selva Kumar Ramasamy [1], Adesh K. Saini [2],
Hardeep Singh Tuli [2], Divya Mittal [3], Aarti Trehan [4]

[1] Department of Chemistry, MMEC, Maharishi Markandeshwar (Deemed to be University), Haryana, India
[2] Department of Bio-Sciences and Technology, MMEC, Maharishi Markandeshwar (Deemed to be University), Haryana, India
[3] Faculty of Agriculture, Maharishi Markandeshwar (Deemed to be University), Haryana, India
[4] Department of Chemistry, Arya Kanya Mahavidyalya, Shahabad Markanda, Haryana, India

ABSTRACT

Introduction and aim. At present, several microbial diseases are prominent and of concern worldwide. The intent of this study was to examine the antibacterial potential of newly synthesized tetradentate macrocyclic complexes against different bacterial strains. The macrocyclic scaffold has gained attention as a biologically active class of supramolecular chemistry due to its unique properties and ability to target various microorganisms. Thus, the goal of the present study was to develop a series of biologically active transition metal-based macrocycles.
Material and methods. All macrocyclic compounds were synthesized by a template method and validated by molar conductivity, elemental studies, and spectral and magnetic studies. Antibacterial activities of all metal complexes were evaluated against *Escherichia coli* (MTCC 739) and *Staphylococcus aureus* (MTCC 731) bacterial strains by taking ampicillin as a standard reference drug. DNA photocleavage potential was explored using agarose gel electrophoresis.
Results. Results revealed the formation of novel macrocyclic complexes via tetra nitrogen bond trapping of metals. Copper complexes have strong potential against *S. aureus* bacteria as copper and nickel both show good DNA photocleavage potential.
Conclusion. The findings endorse the biomedical relevance of these macrocyclic scaffolds, suggesting avenues for further exploration in targeted drug delivery and potential clinical applications. The proposed octahedral geometry for the complexes enhances our understanding of their structural aspects. This research contributes substantively to the field, laying the foundation for future investigations in advanced antimicrobial design and application.
Keywords. anti-bacterial, DFT, DNA photocleavage, molecular docking, template method

Introduction

The profound significance of macrocyclic ligand complexes in physiological processes underscores their pivotal role in recent global research endeavors. These complexes are a prime example of their significance in the complex machinery of living beings, as they are vital to many crucial biological activities.[1–4] The most notable application of the macrocyclic scaffold is in photosynthesis, where chlorophyll, which contains a porphyrin, acts as a pivotal component in absorbing light energy and propelling the synthesis of carbohydrates in plants.

In human biology, macrocyclic derivatives play a major role in the essential movement of oxygen inside cells. The essential protein in red blood cells, he-

moglobin, depends on macrocyclic porphyrin rings that contain iron ions in the center. Because of its structural makeup, hemoglobin may bind oxygen molecules, which makes it easier for oxygen to go from the lungs to tissues and organs. This basic mechanism is essential to the continuation of life. Furthermore, macrocyclic derivatives – especially those that incorporate iron – are essential to the process of cellular respiration. During the energy conversion process, heme groups containing iron ions are used by cytochromes, a type of protein essential to the electron transport chain for electron transfer. This emphasizes how important macrocyclic scaffolds are for supporting several vital biological processes, including respiration.[5,6]

Because of their special qualities and possible uses, heteroatom-containing macrocyclic Schiff-based complexes are a prominent family of molecules in the field of coordination chemistry. The durability and adaptability of supramolecular complexes make them significant. Their capacity to interact with metal ions and their distinct macrocyclic structure make them useful instruments for creating functional molecules with specific characteristics.[5,6]

Because macrocyclic derivatives are distinct in terms of their host-guest chemistry, structure, and behaviors, researchers have been interested in creating new macrocyclic systems. These substances have demonstrated significant promise in a wide range of applications, such as chemical sensors, catalysts, therapeutic agents, agents for magnetic resonance imaging (MRI), and numerous other biomedical uses.[7–9]

Additionally, macrocycles in medicinal chemistry have promise for improving drug development, therapeutic interventions in a range of disorders, and diagnostic procedures. Currently, the varied biological features of the metal complexes of Schiff base macrocycles (including the -C=N group) attract a lot of interest as shown in Figure 1.[10–16]
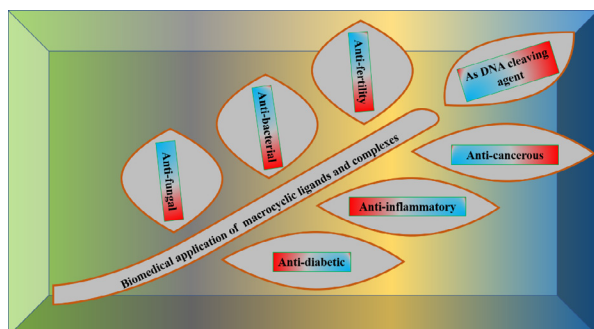
Fig. 1. Biomedical application of Schiff-based macrocyclic ligands and complexes

Aim

Prodded by all the above facts, in this research article, the biological efficacy and synthesis of macrocyclic Ni(II), Co(II), Cu(II), and Zn(II) metal complexes was

carried out. Additionally, computational studies (DFT and molecular docking) have also been used to check the quantum mechanical parameters, molecular mechanisms and binding interactions between the ligands with the active sites of the receptor.

Material and methods

Materials

All solvents and chemicals utilized during synthesis were of AR grade. 1,2-phenylenediamine and maleic anhydride were obtained from SD Fine Chem Ltd, Mumbai, and Sigma-Aldrich respectively. Various metal salts of copper, nickel, cobalt and zinc were procured from Chemigens Research & Fine chemicals, CDH Chemicals, and SD Fine Chem Ltd. All the above chemicals were used as received.

Synthesis of macrocyclic complex

A novel series of tetraazamacrocyclic compounds were synthesized using template cyclization reactions. In a hot methanolic solution of 1,2-phenylenediamine (1.081 g, 10 mmol), divalent metals such as copper, nickel, cobalt, or zinc salts were added (5 millimoles) and dissolved in the least amount of MeOH (methanol). The mixture was then refluxed for nearly an hour. A minor variation in the color of the mixture was a clear indication of the reaction's progress, as it was evidence in favor of metal-amine coordination. Subsequently, to the above solution, a methanolic solution of maleic anhydride (0.9806 g, 10 mmol) was introduced, and refluxing was further continued for about 6–8 hours. The mixture obtained was kept overnight for cooling and precipitation, which was then further filtered and washed with MeOH, ethanol, and diethyl ether, then dried over vacuum (Fig. 2). The yield of the resulting complexes was ~40–60%. The synthesized compounds were soluble in DMSO, DMF, and acetonitrile and insoluble in most common solvents like methanol, ethanol, and chloroform. The proposed synthetic route for complexes has been depicted in scheme (Fig. 2).
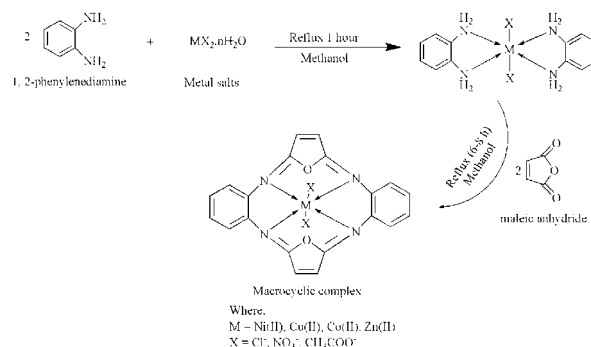
Fig. 2. Reaction procedure for the synthesizing macrocyclic compounds obtained from 1,2-phenylenediamine and maleic anhydride with divalent metal salts of copper, nickel, cobalt, and zinc

Analytical and physical measurements

The determination of the melting point (M.Pt.) was taken on the electrical M.Pt. apparatus. The molar conductivity of complexes was recorded in DMSO on an EI 181 digital conductivity meter available in the laboratory. Magnetic susceptibility measurements were determined at SAIF, IIT, and Roorkee on a vibrating sample magnetometer (Model PAR 155). The IR spectra were taken on a Shimadzu IR spectrometer in the 4000‑400 cm⁻¹ range and 400‑180 cm⁻¹ consuming KBr pellet, and the electronic spectral data were taken on a Shimadzu UV 1800 spectrophotometer at CLIR, MM(DU) Mullana. The CHNS-O-Organic elemental analyzer Flash 2000 series had been used for the elemental analysis at CIL Punjab University, Chandigarh. The NMR spectral data of the divalent zinc complex was taken on a Bruker Advance II 400 NMR spectrometer (400 MHz) in DMSO-d_6 at room temperature, and the mass spectra of the complexes were taken on a Q to F microwater LS-MS at SAIF, Punjab University Chandigarh, India. The powder XRD of the Cu(II) complex was taken on an X-ray diffractometer model X'Pert Pro at SAIF, Punjab University, Chandigarh. Gel electrophoresis cleavage experiments were performed with the help of Axygen electrophoresis supported by a Genei power supply with a potential range of 50–5000 volts.

Biological studies

All the complexes were evaluated for antimicrobial activity, and for initial testing, two of the most prevalent human pathogens were employed, namely *Escherichia coli* (MTCC 739), a fecal contaminant, and *Staphylococcus aureus* (MTCC 731), a predominant Gram-positive human pathogen. In addition, to investigate how the metal complexes exert their influence on microorganisms, an examination of their impact on the genomic DNA (extracted from the respective bacterial strains) was also carried out. In this regard, Gram-negative (*E. coli*) and Gram-positive (*S. aureus*) bacterial strains and plasmid DNA for cleaving studies were sourced from the CLIR, MM(DU) Mullana.

Methods

Anti-bacterial screening

The current screening involves the use of Gram-negative (*E. coli*) and Gram-positive (*S. aureus*) bacterial strains. The evaluation of the antibacterial properties of the metal complexes was conducted through the well diffusion method, employing various concentrations of the complexes (ranging from 100 to 500 µg/mL) dissolved in DMSO as the solvent.[8] The inhibition zone was measured after a 24-hour incubation at temperatures between 35°C and 37°C, as per the experimental conditions.

DNA cleaving studies

Concentrated solutions (100 µg/mL) of the metal complexes were prepared by dissolving them in DMSO. Sub-sequently, all complexes were dissolved in a suspension containing Tris, EDTA (TE) buffer, and plasmid DNA. These reaction solutions were carefully prepared in polyethylene micro-centrifuge tubes and then exposed to UV irradiation (265 nm) for a duration of 25 minutes on the surface of a transilluminator. To create the gel matrix, 1 g of agarose was dissolved in 100 ml of 1×TAE buffer. Once the temperature reached approximately 55°C, ethidium bromide (5 mg/0.5 mL) was added to the mixture. This resulting mixture was then transferred into a gel cassette equipped with a comb and allowed to solidify. Subsequently, it was placed in an electrophoresis chamber filled with TAE buffer. For the electrophoresis procedure, all samples were mixed with loading dye and carefully loaded into wells alongside untreated DNA samples. Electrophoresis was conducted for a duration of one and a half hours, after which the bands were visualized under a transilluminator.[17,18]

Computational studies

Computational methods

All calculations were made using Gaussian 09 (G 09) computational codes applying B3LYP (Becke's three-parameter hybrid exchange and Lee-Yang-Parr non-local correlation functional) using DFT (density functional theory).[19] For all computations, standard 6-31G (d,p) basis set for the lighter element such as C, H, N and O and the LanL2DZ effective core potential for metals i.e. Co, Cu, Ni and Zn apply.[20] All geometries will be optimized to zero negative vibrational-frequency to signify local minima accompanying with the positive eigen values only. To account for solvent effect, DFT calculations are coupled with CPCM (conductor-like polarizable continuum model) in a water medium.[21]

Docking methods

Lead molecules were manifest to molecular docking studies using AutoDoc 4, which covers the Lamarckian Genetic Algorithm (LGA) to calculate the binding affinities of some conformers and AutoDoc Tools (ADT) to perform operations and resulting calculations.[22] The three-dimensional structures of complexes S1, S2, S3, S4, S5, S6, S7, S8 and S9 obtained for DFT optimized geometries were converted to PDB form through Gauss View. The optimized complexes with the X-ray crystal structure of COX-2 (PDB ID: 5COX) were used for docking purposes.[22] Each atom in both case the target and the lead compounds were imbued with Gasteiger charges. Prior to docking, a grid size of 40×40×40 for the protein was assigned to the binding site, the number of points in x, y, and z were used with a spacing of 1 Å to represent all putative active site residues that most prominent are HIS886 and HIS386.[22] The functioning principle and output parameters were similar to the aforementioned DNA docking. Docked poses are visualized by PyMol and LigPlot+ molecular visual programs.[23]

Results

(S1) $[Cu(C_{20}H_{12}N_4O_2)(OAc)_2]$: Yield ~ 58%, Color=Black, M.wt.=522, M. pt.=265°C; Analytical Calculation: M=11.11; C=53.07; H=2.85; N=9.69; O=17.34; Molar conductivity in DMSO 15 ohm^{-1} cm^2 mol^{-1}. Magnetic moment μ_{eff} (BM): 1.86. IR (cm^{-1}): $v_{C=N}$, 1550 (s); v_{C-N}, 1260 (s); $v_{M\rightarrow N}$, 420 (s); v_{OAc}, 1280 (m). UV-visible in DMSO (nm): ~990, ~680, ~320.

(S2) $[Cu(C_{20}H_{12}N_4O_2)Cl_2]$: Yield ~ 60%, Color=Brown, M.wt.=475, M. pt.=260°C; Analytical Calculation: M=11.35; C=49.55; H=2.12; N=10.77; O=5.71; Molar conductivity in DMSO 13 ohm^{-1} cm^2 mol^{-1}. Magnetic moment μ_{eff} (BM): 1.90. IR (cm^{-1}): $v_{C=N}$, 1530 (s); v_{C-N}, 1310 (s); $v_{M\rightarrow N}$, 425 (s); v_{M-X}, 350 (m). UV-visible in DMSO (nm): ~990, ~680, ~480, ~310.

(S3) $[Cu(C_{20}H_{12}N_4O_2)(NO_3)_2]$: Yield ~ 59%, Color=Lavender blue, M.wt.=527, M. pt.=270°C; Analytical Calculation: M=11.01; C=40.29; H=2.09; N=14.92; O=22.25; Molar conductivity in DMSO 18 ohm^{-1} cm^2 mol^{-1}. Magnetic moment μ_{eff} (BM): 1.91. IR (cm^{-1}): $v_{C=N}$, 1525 (s); v_{C-N}, 1315 (s); $v_{M\rightarrow N}$, 450 (s); v_{M-X}, 230 (m). UV-visible in DMSO (nm): ~1000, ~700, ~490, ~310.

(S4) $[Ni(C_{20}H_{12}N_4O_2)Cl_2]$: Yield ~ 41%, Color=White, M.wt.=470, M. pt.=243°C; Analytical Calculation: M=11.49; C=50.12; H=2.17; N=10.92; O=5.81; Molar conductivity in DMSO 16 ohm^{-1} cm^2 mol^{-1}. Magnetic moment μ_{eff} (BM): 3.05. IR (cm^{-1}): $v_{C=N}$, 1515 (s); v_{C-N}, 1280 (s); $v_{M\rightarrow N}$, 430 (s); v_{M-X}, 280 (m). UV-visible in DMSO (nm): ~810, ~310, ~240.

(S5) $[Ni(C_{20}H_{12}N_4O_2)(NO_3)_2]$: Yield ~ 54%, Color=Purple, M.wt.=522, M. pt.=240°C; Analytical Calculation: M=10.22; C=43.93; H=1.99; N=15.07; O=22.47; Molar conductivity in DMSO 18 ohm^{-1} cm^2 mol^{-1}. Magnetic moment μ_{eff} (BM): 3.10. IR (cm^{-1}): $v_{C=N}$, 1510 (s); v_{C-N}, 1270 (s); $v_{M\rightarrow N}$, 425 (s); v_{M-X}, 215 (m). UV-visible in DMSO (nm): ~800, ~430, ~320, ~280.

(S6) $[Co(C_{20}H_{12}N_4O_2)(OAc)_2]$: Yield ~ 45%, Color=Moss green, M.wt.=517, M. pt.=275°C; Analytical Calculation: M=10.39; C=54.72; H=3.01; N=9.83; O=17.56; Molar conductivity in DMSO 18 ohm^{-1} cm^2 mol^{-1}. Magnetic moment μ_{eff} (BM): 4.31. IR (cm^{-1}): $v_{C=N}$, 1520 (s); v_{C-N}, 1320 (s); $v_{M\rightarrow N}$, 425 (s); v_{OAc}, 1230 (m). UV-visible in DMSO (nm): ~780, ~510, ~320.

(S7) $[Co(C_{20}H_{12}N_4O_2)Cl_2]$: Yield ~ 52%, Color=Dark orange, M.wt.=470, M. pt.=270°C; Analytical Calculation: M=11.53; C=49.09; H=2.01; N=10.92; O=5.81; Molar conductivity in DMSO 15 ohm^{-1} cm^2 mol^{-1}. Magnetic moment μ_{eff} (BM): 3.99. IR (cm^{-1}): $v_{C=N}$, 1540 (s); v_{C-N}, 1290 (s); $v_{M\rightarrow N}$, 440 (s); v_{M-X}, 290 (m). UV-visible in DMSO (nm): ~790, ~520, ~310.

(S8) $[Co(C_{20}H_{12}N_4O_2)(NO_3)_2]$: Yield ~ 56%, Color=Dark orange, M.wt.=523, M. pt.=265°C; Analytical Calculation: M=10.26; C=44.91; H=2.01; N=15.06; O=23.46; Molar conductivity in DMSO 19 ohm^{-1} cm^2 mol^{-1}. Magnetic moment μ_{eff} (BM): 4.15. IR (cm^{-1}): $v_{C=N}$, 1525 (s); v_{C-N}, 1330 (s); $v_{M\rightarrow N}$, 435 (s); v_{M-X}, 230 (m). UV-visible in DMSO (nm): ~730, ~540, ~320.

(S9) $[Zn(C_{20}H_{12}N_4O_2)(OAc)_2]$: Yield ~ 51%, Color=Moss green, M.wt.=524, M. pt.=254°C; Analytical Calculation: M=11.48; C=53.03; H=3.02; N=9.70; O=17.33; Molar conductivity in DMSO 20 ohm^{-1} cm^2 mol^{-1}. Magnetic moment μ_{eff} (BM): 0.0. IR (cm^{-1}): $v_{C=N}$, 1560 (s); v_{C-N}, 1325 (s); $v_{M\rightarrow N}$, 445 (s); v_{OAc}-, 1250 (m). UV-visible in DMSO (nm): ~470, ~280. NMR (DMSO, in ppm): δ, 7.6 (m, benzene ring); 6.7 (m, furan ring); 2.50 (s, acetate ion).

ESI-MS (m/z): Mass spectral data (MS) of metal compounds were noted, as this technique provides the structural evidence of compounds under analysis. The polymeric or monomeric character of macrocyclic compounds can be interpreted with the help of MS technique.[24] The MS of some representative complexes S1, S2, S3, S5, S7, S8, and S9 showed molecular ion peaks at 521.97, 474.32, 526.08, 521.96, 469.12, 524.43, and 523.48 corresponding to [M]$^+$ ion peaks respectively. The MS of S1 exhibits peaks at 523.47 and 540.53 corresponding to [M+1]$^+$ and [M+H$_2$O]$^+$ ion peaks respectively. The MS of S2 complex exhibit molecular ion peak at m/z 475.01 and 473.32 corresponds to [M+1]$^+$ and [M-H]$^+$ ion respectively. [M+DMSO]$^+$ ion peak exhibited by S3 and S8 at m/z 607.39 and 601.59 respectively.

Powder X-ray diffraction

In the absence of a single crystal system, the powder X-ray diffraction methodology is a well-liked method for analyzing the structural data of inorganic and organic materials. In this study, a powder X-ray diffraction analysis of one of the Cu(II) metal complex was carried out by scanning it between Bragg's angle 2θ=5° and 90°. The $[Cu(C_{20}H_{12}N_4O_2)(NO_3)_2]$ produced shows several sharp and intense diffraction peaks at 2θ value of 8.57°, 20.83°, 22.46°, 25.92°, 30.23°, 33.69° that indicate its crystalline form in the diffractogram of the complex. Peak positions show the value of 2θ that are corresponds to the interatomic spaces present in crystal lattice. Higher the intensity of the peak more is the number of atoms in particular arrangement in the lattice site that related to the strength of scattering.[25,26]

Antibacterial assay

All the novel macrocyclic complexes were screened for their anti-bacterial potential against *E. coli* (Gram-negative) and *S. aureus* (Gram-positive). Ampicillin is taken as standard reference drug for elucidation of bactericidal effect of synthesized macrocyclic scaffold on Gram-negative bacteria and Gram-positive bacteria. All complexes showed no activity against *E. coli* (Gram-negative) tested strains as shown in Fig. 3 (not shown in tabular form), where strong activity was observed against *S. aureus* (Gram-positive bacteria) as shown in Figures 4, 5, and Table 1.
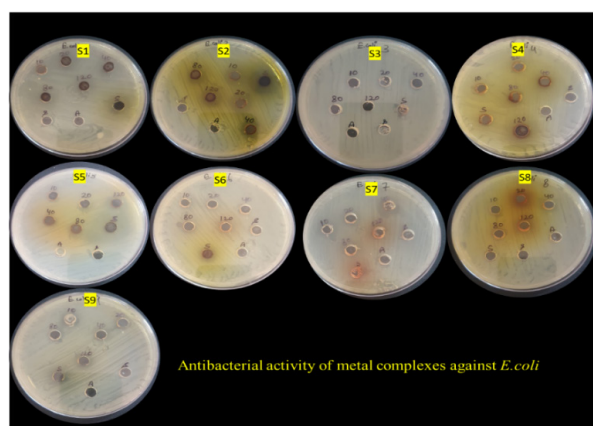
Fig. 3. Antibacterial activity of macrocyclic complexes against *E. coli* (Gram-negative bacteria)
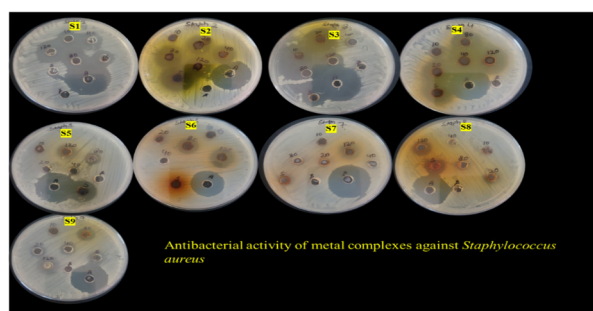
Fig. 4. Anti-bacterial activity of metal complexes against *S. aureus* (Gram-positive bacteria)

Table 1. Zone of inhibition diameter of novel metal complexes against (Gram-positive bacteria)*

Sample name	Zone diameter measurement at different concentrations of the metal complexes (in mm)					
	100 µg/mL	200 µg /mL	300 µg/mL	400 µg/mL	500 µg/mL	Drug (Vancomycin)
S1	0	12	12	17	17	30
S2	12	15	20	20	25	30
S3	12	16	20	20	25	30
S4	4	12	19	20	25	30
S5	0	0	0	6	10	30
S6	0	0	0	8	12	31
S7	0	0	0	0	10	30
S8	0	2	0	5	10	30
S9	0	3	3	9	12	35

* values – means of three replicates (including the diameter of the well)

DNA photo-cleavage studies

The most tenacious concern for humanity today is the potential conquest of cancer through the discovery of chemical nucleases. Transition metal complexes, known for their significant nuclease activities and specific DNA binding capabilities, have been investigated for their impact on DNA photocleavage.[27] The results of the DNA photocleavage analysis are depicted in Figure 6.
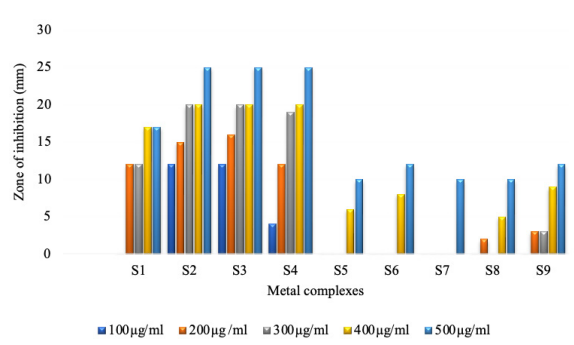
Fig. 5. Bar graph representation of zone of inhibition diameter of novel metal complexes against Gram-positive bacteria
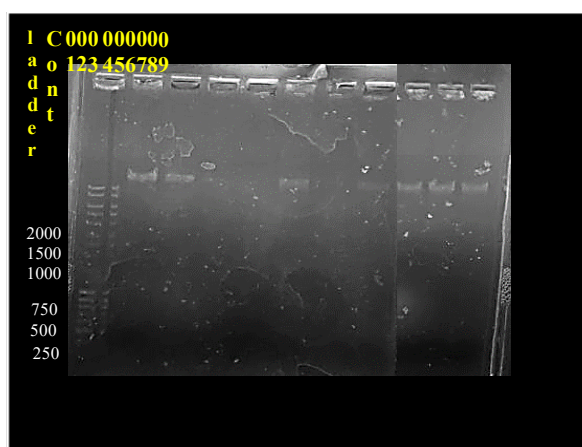
Fig. 6. DNA photo-cleavage study against metal complexes indicated S2 and S3, S5 exhibit strong DNA photo-cleavage activity, S4 and S6 showed moderate cleavage of DNA whereas S7, S8, S9 showed no DNA cleavage

DFT studies

Computational studies of synthesized *d*-metal complexes such as S1-S9 complex were carried out by using the combined DFT-B3LYP technique by means of Gaussian-09 computational codes. Various parameters of quantum-chemical were computed through B3LYP/6-31G**/LanL2DZ ECP techniques i.e. geometry optimization, ESP charges, molecular energy, the energy of FMO (frontier molecular orbitals), and bandgap etc. The square planar geometry exhibited by the macrocyclic complexes as shown in Figure 7. The ligand describes the square planar geometry with d metals (Co (II), Ni(II), Cu (II) and Zn(II)) center the corresponding key bond - lengths of the N---M and O---M was found to be 2.427, 2.506, 2.472, 2.445 Å and 1.799, 1.822, 1.760, 1.862 Å for Co(II) complexes (S6-S8), Ni(II) complexes (S4-S5), Cu(II) complexes (S1-S3), and Zn(II) complex S9 respectively (Table 2). Electrostatic potential recorded onto the surface of constant electron density for optimized geometry on the Van der Walls surface. Also, it is very beneficial in exploration of molecular structures with their photophysical properties relationship, as well

as hydrogen-bonding interaction in d-metal complexes such as S1-S9.[28] The maximum negative region that is showed by red color, is the favored site for the electrophilic attack, and the maximum positive region is shown blue color that is favored site for the nucleophilic attack (Fig. 8).
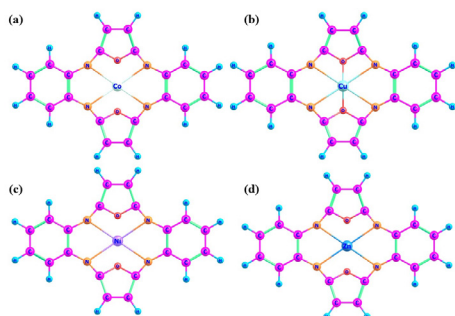
Fig. 7. Optimized molecular geometry S6-S8(a), S1-S3(b), S4-S5(c), and S9(d) complex by using the DFT/B3LYP method
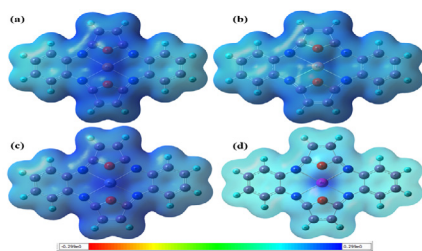
Fig. 8. Electrostatic potential map of S6-S8(a), S1-S3(b), S4-S5(c), and S9(d) complex by using the DFT/B3LYP method

Table 2. The optimized bond length of tetrahedral complexes (Å)

S. No	Complex ID	N_1---M	N_2---M	N_3---M	N_4---M	O_1---M	O_2---M
1	S1-S3	2.506	2.506	2.506	2.506	1.822	1.822
2	S4-S5	2.472	2.472	2.472	2.472	1.760	1.760
3	S6-S8	2.427	2.427	2.427	2.427	1.799	1.799
4	S9	2.445	2.445	2.445	2.445	1.862	1.862

The FMO (frontier molecular orbital) comparing the HOMO (Highest occupied molecular orbital), and the LUMO (lowest molecular orbital) with energy gap (ΔE) between the HOMO and the LUMO of all the d-complex such as S1-S9 are derivatives were calculated and displayed in Fig. 9. Energies of the FMOs (E_{HOMO} and E_{LUMO}), ΔE which describes the eventual C→T interaction within the molecule, chemical potential (μ), electronegativity (χ), global softness (S), global hardness (η) and global electrophilicity index (ω) are recorded in Table 3.[29,30] The importance of all these parameters is to calculate the molecular reactivity and stability. The electrophilicity index i.e. ω is one of the vital quantum chemical parameter, which describes the poisonousness of numerous pollutants in terms of their site selectivity

and reactivity.[31] Also, the electrophilicity calculates the biological potency of drug receptor interaction.
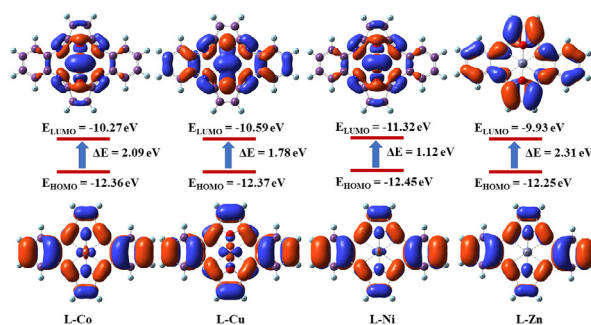
Fig. 9. FMOs of S6-S8(L-Co), S1-S3(L-Cu), S4-S5(L-Ni) and S9(L-Zn) complex by using DFT/B3LYP method

Table 3. Calculated molecular electronic parameters*

S. No	Complex	Energy (kcal/mol)	DM	HOMO (eV)	LUMO (eV)	Gap (eV)	χ (eV)	μ (eV)	η (eV)	S (eV)	ω (eV)
1	S1-S3	-840655.94	3.38	-12.37	-10.59	-1.78	11.48	-11.48	-0.89	-0.44	-58.60
2	S4-S5	-823542.95	1.84	-12.45	-11.32	-1.12	11.89	-11.89	-0.56	-0.28	-39.69
3	S6-S8	-808295.64	1.58	-12.36	-10.27	-2.09	11.31	-11.31	-1.05	-0.52	-66.95
4	S9	-758251.46	1.72	-12.25	-9.93	-2.31	11.09	-11.09	-1.16	-0.58	-71.08

* DM – dipole moment, EH – energy of HOMO, EL – energy of LUMO, ΔE – energy band gap, χ – electronegativity, μ – chemical potential, η – global hardness, S – global softness, ω – global electrophilicity index

Molecular modelling studies

A molecular docking study is significant for forecasting the molecular mechanism and binding interaction between the active site of the receptor and ligand. Molecular docking studies of macrocyclic compounds, S1-S9, in potent area of the COX-2 (PDB code is 5COX), were completed, to get a perception into the nature of the interaction between the complex and potent site of 5COX, with AutoDock4 tool. The valuation of every docked molecule was completed by assessing the scoring function as shown in Table 4, which assists as evidence of how finely the ligand-bound inside the binding pocket.

It was found that all of the complexes had fitness docking scores ranging from -7.27 to -8.08, with the medication celecoxib having a value of -5.10 (Table 4). Among all the substances, compound zinc acetate-based (S9) placed first with a docking score of -8.08 and binding energy of 8.06 kcal/mol, and Ni(II)-based (S4-S5) placed second with a docking score of -8.01 and binding energy of 8.00 kcal/mol whereas celeoxib had a docking score of -5.10 and binding energy of -6.00. Furthermore, the compounds S1, S3, and S9 exhibit hydrogen bonding interactions with the HIS207 residue, with bond lengths of 3.26, 3.09, and 3.09, respectively. It also demonstrated excellent interactions with target protein binding site residues in a fashion similar to celecoxib. Fig 10 depicts the protein-ligand interaction visualization of all compounds and the medication celecoxib.

Fig 11 depicts the 3D binding surface plot of all compounds and drugs with protein. Overall, the docking data demonstrate that the synthesized complexes outperform the conventional medication celecoxib in terms of binding interaction with COX2.
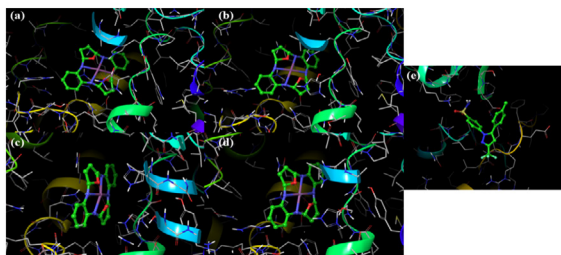
Fig. 10. Molecular docking interaction of S1-S9 complexes with COX2
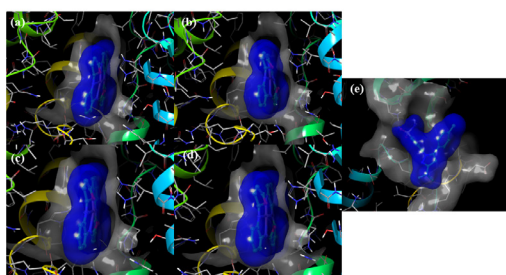
Fig. 11. Ligplot 2D residues interaction plot of S1-S9 complexes with COX2

Table 4. Molecular docking studies of S1-S9 complexes with COX2

Complex	Binding free energy ($\Delta G_{binding}$)$^\alpha$	Vdw_hb_desolv energy ($\Delta G_{vdW+hb+desolv}$)	Electrostatic energy (ΔG_{elec})	Total internal energy (ΔG_{total})	Torsional free energy (ΔG_{tor})	H bond length (Å)	Interaction residue
S1-S3	-7.79	-7.77	-0.02	0.0	0.0	3.26	HIS207
S4-S5	-8.01	-8.00	-0.01	0.0	0.0	--	--
S6-S8	-7.27	-7.28	0.01	0.0	0.0	3.09	HIS207
S9	-8.08	-8.06	-0.02	0.0	0.0	3.09	HIS207
Cele	-5.10	-6.00	-0.3	-0.84	1.19	2.62, 2.66	ASP393, LYS405

Discussion

The analysis of metal complexes shows that the molecular formula of synthesized complexes can be $[M(C_{20}H_{12}N_4O_2)X_2]$; where M are metals i.e. divalent copper, cobalt, nickel and zinc metals and X=CH_3COO^-, Cl^-, and NO_3^-. The monomeric character of metal complexes was affirmed through molecular weight measurement and ESI-MS studies. Molar conductivity of complexes was checked in DMSO which lies in range of 12-20 ohm^{-1} cm^2 mol^{-1} that indicates the non-electrolytic nature of the complexes.[32] It was observed that the pair of bands which exist between 3,200-3,400 cm^{-1} in the spec-

trum of 1,2-phenylenediamine which is due to ν(-NH$_2$) were found missing in IR of all synthesized complexes.[8] Moreover, the absence of strong absorption band near about 1,710-1,720 cm^{-1} shows disappearance of $\nu_{(-C=O)}$ group due to maleic anhydride.[33] Furthermore, the appearance of a medium to a sharp absorption band in range 1,550-1,640 cm^{-1} provides strong evidence for condensation of carbonyl group of maleic anhydride with amine group of 1,2-phenylenediamine, and is also ascribed to the formation of azomethine (-C=N) linkage. Slight drifting in absorbance frequency was also observed due to the coordination of N of ligand with the central metal ion of synthesized metal complexes. The medium to strong intensity band existing near 1,266-1,342 cm^{-1} can be ascribed to $\nu_{(C-N)}$ vibrations. IR spectra for all nitrate complexes at 1,010- 1,030 cm^{-1}, 1,290-1,320 cm^{-1}, and 1,408- 1,440 cm^{-1} suggest that the nitrate group of metal nitrate salts are coordinated in unidentate fashion with a central metal ion.

Presence of bands in regions 1,650-1,680 cm^{-1} and 1,258-1,290 cm^{-1} can be ascribed to asymmetric $\nu_{(COO-)}$ stretching vibration and symmetric $\nu_{(COO-)}$ stretching vibration of acetate ions of acetate metal salts respectively.[34] IR spectra of far infrared regions show bands at 420-450 cm^{-1} with respect to $\nu_{(M-N)}$ vibration. All synthesized macrocyclic metal complexes show bands in the 420-450 cm^{-1} region, this identifies the co-ordination of azo-methine nitrogen to copper, cobalt, nickel or zinc metal. Absorption band present in region 220-250 cm^{-1} and 300-350 cm^{-1} can be attributed to the $\nu_{(M-O)}$ stretching vibration of nitrate complexes and the $\nu_{(M-Cl)}$ vibrations respectively.[32]

Electronic spectrum of synthesized macrocyclic compounds was reported at room temperature in solution state by using DMSO as solvent. Absorbance band at ~720-790, ~500-540 and 310-320 nm can be corresponds to the $^4T_{1g} \rightarrow {}^4T_{2g}$ (F), (ν_1); $^4T_{1g} \rightarrow {}^4A_{2g}$ (F), (ν_2); and $^4T_{1g}$ (F) $\rightarrow {}^4T_{1g}$(P), (ν_3) electronic transition exhibited by Co(II) metal complexes which is similar to reported distorted octahedral geometry, whereas Ni(II) metal complexes exhibited bands at ~800-820, ~420-430, ~310-320 and ~240-280 nm which can be ascribed to the $^3A_{2g} \rightarrow {}^3T_{2g}$ (F), $^3A_{2g} \rightarrow {}^3T_{1g}$ (F), $^3A_{2g} \rightarrow {}^3T_{1g}$ (P) and n-π* transitions respectively and show the presence of octahedral environment.[35-37] Magnetic moment (μ_{eff}) of divalent nickel complexes lies in range of 3.05-3.10 B.M. which exhibit the presence of two unpaired electrons.[8] In the case of Cu(II) metal complexes absorbance band exhibits at ~990-1010, ~660-680, ~480-490, and ~310-320 nm corresponding to various d-d transition bands while π→π* transition band appeared at 240-290 nm and exhibit these complexes have distorted octahedral environment.[33] The effective magnetic moment of Co (II) and Cu (II) complexes was found in variation of 3.99-4.31, and 1.86-1.91 B.M. respectively.[36] The divalent zinc metal compound is

exhibiting an absorbance band near ~470-480 and ~280-300 nm, which may be easily assigned to n→π* and π→π* transition resp.[37,38] ^{1}H-NMR (nuclear magnetic resonance) spectrum of the $[Zn(C_{20}H_{12}N_4O_2)(OAc)_2]$ complex exhibited no peak with respect to the free amine (-NH$_2$) protons which indicate the complex formation.[8] Diffractogram of $[Cu(C_{20}H_{12}N_4O_2)(NO_3)_2]$ produced shows several sharp and intense diffraction peaks at 2θ value of 8.57°, 20.83°, 22.46°, 25.92°, 30.23°, 33.69° that indicate its crystalline form of the complex. The Debye Scherrer formula, D=Kλ/βcosθ (where D is normal or average crystallite size, K is Scherrer constant, λ(0.15406) is the employed for X-ray wavelength, and β is the full width half maximum), has been used to forecast the normal crystallite size from notable peaks.[39] The complex $[Cu(C_{20}H_{12}N_4O_2)(NO_3)_2]$ has a crystallite size of 28.98 nm, which denotes the coordinated compounds with nanocrystalline phase.

An urgent need exists for research into anti-infectious agents. Infectious disease outbreak rates have been seen to be rising in recent years. The WHO finds that new antibiotics that target pathogenic microorganisms may not only assist to reduce infections-related fatalities but also lessen the threat of microbes that are treatment resistant. In this regard antibacterial potential of synthesized macrocyclic complexes were also exposed, which exhibits strong activity against *S. aureus* (Gram-positive bacteria) by metal complexes S2, S3, and S4 in concentration range 100–500μg/mL. On the other hand, S1, S5, S8, and S9 showed moderate activity and showed maximum potential to inhibit bacteria at 200 μg/mL dose. There was no activity noticed in the case of complex S6 and S7. The findings of DNA photocleavage studies indicate that metal complexes containing Cu(II) metal ions, such as S2 and S3, as well as Ni(II) metal ions like S5, exhibit robust DNA photocleavage activity. In contrast, the macrocyclic complex featuring divalent nickel metal ions, S4, and divalent cobalt metal ions, S6, demonstrate a moderate level of DNA cleavage. On the other hand, S7, S8 and S9 do not exhibit any DNA cleavage activity. Previously it has been reported that macrocyclic complexes are known to possess promising antibacterial potential. For instance – Rathi et al. reported bioactive macrocyclic complexes against various gram positive and gram-negative bacterial strains in the range of 64- 512μg/mL dose. Therefore, our results are consistent with the previously reported studies.[37,38]

DFT studies describes the square planar geometry of ligand with d metals (Co (II), Ni(II), Cu (II) and Zn(II)) center. As shown in Fig. 9, the LUMO orbitals are placed on the center of metal and the HOMO orbitals are placed on the ligand system in case of Co²⁺, Ni²⁺ and Cu²⁺. But in the case of Zn²⁺ the LUMO orbital is placed on ligand system, showing partially filled d-metal center can act as an excited electron ac-

ceptor and filled Zn act as no involving of acceptor. Both complexes exhibit the band gap energy range from 1.12 to 2.31 eV. Furthermore, ΔE is a prime parameter for the characterization of kinetic stability and chemical reactivity of the molecule.[40] ΔE is small which designates easy charge transfer (C→T) process in it, which influences the biological potency of the molecule. The findings of molecular docking studies reveals Ni(II) complexes (S4-S5) and Zn(II) complex (S9) both were designated to be extremely active with their uppermost docking scores, i.e., -8.01 kcal/mol and -8.08 kcal/mol respectively. The Co(II) complexes (S6-S8), Cu(II) complexes (S1-S3), and Zn(II) complex (S9) show one hydrogen bonding with HIS207, and hydrogen bonds length was found to be 3.09 Å and 3.29 Å.

Conclusion

Because infection and mortality rates from microbiological diseases are rising so rapidly in the modern era, modern medicine faces enormous challenges. This work synthesized a unique series of macrocyclic compounds with the Schiff bases Ni(II), Co(II), Cu(II), and Zn(II). Analytical and spectroscopic results demonstrated the macrocyclic complex's monomeric nature. Diffractogram analyses have revealed that a complex with a dimension of 28.98 nm is nanocrystalline. The synthetic complexes' ability to cleave DNA and fight germs was assessed. At 200 μg/mL, all complexes exhibited excellent to moderate antibacterial efficacy, while macrocycles had strong DNA-cleaving potency. Due to their highest docking scores, docking studies demonstrate the extremely active behavior of both Ni(II) and Zn(II) complexes towards the active region of COX-2 through their uppermost docking score i.e. -8.01 kcal/mol and -8.08 kcal/mol respectively.

Conflict of interest
The authors state, there are no conflict of interest about the publication of this research work.

Data availability
The dataset generated during research work is available from corresponding author on request.

Ethics approval
Not applicable.

References

1. Jain S, Rana M, Sultana R, Mehandi R, Rahisuddin. Schiff Base Metal Complexes as Antimicrobial and Anticancer Agents. *Polycycl Aromat Compd*. 2023;43(7):6351-6406. doi: 10.1080/10406638.2022.2117210

2. Kamboj M, Singh DP, Singh AK, Chaturvedi D. Molecular modeling, in-silico docking and antibacterial studies of novel template wangled macrocyclic complexes involving isatin moiety. *J Mol Struct*. 2020;1207:127602. doi: 10.1016/j.molstruc.2019.127602

3. Kaczmarek MT, Zabiszak M, Nowak M, Jastrzab R. Lanthanides: Schiff base complexes, applications in cancer diagnosis, therapy, and antibacterial activity. *Coord Chem Rev*. 2018;370:42-54. doi: 10.1016/j.ccr.2018.05.012

4. O'Riley HA, Levina A, Aitken JB, Lay PA. Synthesis, reactivities and anti-cancer properties of ruthenium(II) complexes with a thiaether macrocyclic ligand. *Inorganica Chim Acta*. 2017;454:128-138. doi: 10.1016/j.ica.2016.07.050

5. Sangwan V, Singh DP. In-vitro DNA binding and antimicrobial studies of trivalent transition metal ion based macrocyclic complexes. *Vietnam J Chem*. 2019;57(5):543-551. doi: 10.1002/vjch.201900058

6. Sangwan V, Singh DP. Synthesis, biological and molecular modeling studies of macrocyclic complexes of trivalent metal ions. *Iran Chem Commun*. 2017;5(0):345-351.

7. Mishra P, Sethi P, Sharma N, Sharma J. Macrocyclic scaffold: A boon in advancement of sensor technology- Review. *Mater Today Proc*. 2022;71(2):370-376. doi: 10.1016/j.matpr.2022.09.448

8. Sangwan V, Singh DP. Macrocyclic Schiff base complexes as potent antimicrobial agents: Synthesis, characterization and biological studies. *Mater Sci Eng C*. 2019;105:110119. doi:10.1016/j.msec.2019.110119

9. Purti M, Pooja S, Anjana K. Emerging applications and host- guest chemistry of synthetic macrocycles. *Res J Chem Environ*. 2022;26(7):153-167.

10. Pradhan A, Kumar A. A review: An overview on synthesis of some Schiff bases and there metal complexes with anti-microbial activity. *Chem Process Eng Res*. 2015;35(Ii):84-87.

11. Kajal A, Bala S, Kamboj S, Sharma N, Saini V. Schiff Bases: A Versatile Pharmacophore. *J Catal*. 2013;2013(Mic):1-14. doi: 10.1155/2013/893512

12. Sharma K, Agarwal S, Gupta S. Antifungal, antibacterial and antifertility activities of biologically active macrocyclic complexes of Tin(II). *Int J ChemTech Res*. 2013;5(1):456-463.

13. Zhang Z, Wang H, Wang Q, et al. Anticancer activity and computational modeling of ternary copper (II) complexes with 3-indolecarboxylic acid and 1,10-phenanthroline. *Int J Oncol*. 2016;49(2):691-699. doi: 10.3892/ijo.2016.3542

14. Chandra S, Agrawal S. Spectroscopic characterization of Lanthanoid derived from a hexadentate macrocyclic ligand: Study on antifungal capacity of complexes. *Spectrochim Acta - Part A Mol Biomol Spectrosc*. 2014;124(14):564-570. doi: 10.1016/j.saa.2014.01.042

15. Ibrahim M, Nabi HU, Muhammad N, et al. Synthesis, Antioxidant, Molecular Docking and DNA Interaction Studies of Metal-Based Imine Derivatives. *Molecules*. 2023;28(15):5926. doi: 10.3390/molecules28155926

16. Hazarika B, Singh VP. Macrocyclic supramolecular biomaterials in anti-cancer therapeutics. *Chinese Chem Lett*. 2023:108220. doi: 10.1016/j.cclet.2023.108220

17. Khare R, Sethi P. Studies and antibacterial properties Innovare Properties. *Int J Pharm Pharm Sci*. 2015;7(7):1-8.

18. Pooja S, Pernita D, Gupta GK, Mostafa Sahar I, Simrat K. Synthesis, characterization, anti-bacterial and DNA nicking activity of new complexes of 1-(2,4-dinitrophenylamino)- 4, 4, 6-trimethyl- 3, 4-dihydropyrimidine-2-(1H)--thione. *Res J Chem Environ*. 2018;22(11):73-88.

19. Jana S. Assessment and Benchmarking of Proposed Exchange-Correlation Approximations in Density Functional Theory. http://idr.niser.ac.in:8080/jspui/handle/123456789/200. Accessed April 5, 2023.

20. Kruse H, Goerigk L, Grimme S. Why the standard B3LYP/6-31G* model chemistry should not be used in DFT calculations of molecular thermochemistry: Understanding and correcting the problem. *J Org Chem*. 2012;77(23):10824-10834. doi: 10.1021/jo302156p

21. Ghiggino KP, Scully AD, Leaver IH. Effect of solvent on excited-state intramolecular proton transfer in benzotriazole photostabilizers. *J Phys Chem*. 1986;90(21):5089-5093.

22. Tamanna, Fu C, Qadir M, et al. Thiadiazine thione derivatives as anti-leishmanial agents: synthesis, biological evaluation, structure activity relationship, ADMET, molecular docking and molecular dynamics simulation studies. *J Biomol Struct Dyn*. 2023:1-15 doi: 10.1080/07391102.2023.2245480

23. Wallace AC, Laskowski RA, Thornton JM. Ligplot: A program to generate schematic diagrams of protein-ligand interactions. *Protein Eng Des Sel*. 1995;8(2):127-134. doi: 10.1093/protein/8.2.127

24. Keypour H, Mahmoudabadi M, Shooshtari A, et al. Synthesis and characterization of two new macroacyclic Schiff-base ligands containing piperazine moiety and mononuclear Co(III) and Cu(II) complexes, spectral, X--ray crystal structural, theoretical studies, cytotoxic and antibacterial properties. *Polyhedron*. 2017;129(3):189-198. doi: 10.1016/j.poly.2017.03.035

25. Cheng J, Xuan X, Yang X, Zhou J, Cen K. Preparation of a Cu(BTC)-rGO catalyst loaded on a Pt deposited Cu foam cathode to reduce CO2 in a photoelectrochemical cell. *RSC Adv*. 2018;8(56):32296-32303. doi: 10.1039/c8ra05964k

26. Gull P, Malik MA, Dar OA, Hashmi AA. Design, synthesis and spectroscopic characterization of metal (II) complexes derived from a tetradentate macrocyclic ligand: Study on antimicrobial and antioxidant capacity of complexes. *Microb Pathog*. 2017;16(6):882-894. doi: 10.1016/j.micpath.2017.01.036

27. Sethi P, Khare R, Choudhary R. Complexes of pyrimidine thiones: Mechanochemical synthesis and biological evaluation. *Asian J Chem*. 2020;32(10):2594-2600. doi: 10.14233/ajchem.2020.22813

28. Scrocco E, Tomasi J. Electronic Molecular Structure, Reactivity and Intermolecular Forces: An Euristic Interpretation by Means of Electrostatic Molecular Potentials. *Advances in Quantum Chemistry*. 1978;11:115-193. doi: 10.1016/S0065-3276(08)60236-1

29. Pearson RG. Quantum mechanical parameters. *J Org Chem*. 1989;54:1423-1430.

30. Padmanabhan J, Parthasarathi R, Elango M, Subramanian BS, Krishnamoorthy S. Electron spray. *J Phys Chem A*. 2007:1358-1358.

31. Parathasarathi R, Padmanabhan J, Subramaniam V, Sarkar U, Malti B, Chattaraj P. Internet electron. *J Mol Des*. 2003;2:798-813.

32. Rathi P, Singh DP. Template engineered biopotent macrocyclic complexes involving furan moiety : Molecular modeling and molecular docking. *J Mol Struct*. 2015;1093:201-207. doi: 10.1016/j.molstruc.2015.03.045

33. Rathi P, Singh DP, Surain P. Synthesis, characterization, powder XRD and antimicrobial-antioxidant activity evaluation of trivalent transition metal macrocyclic complexes. *Comptes Rendus Chim*. 2015;18(4):430-437. doi: 10.1016/j.crci.2014.08.002

34. Singh DP, Grover V, Rathi P, Jain K. Trivalent transition metal complexes derived from carbohydrazide and dimedone. *Arab J Chem*. 2017;10:1795-1801. doi: 10.1016/j.arabjc.2013.07.004

35. Zeynali H, Keypour H, Hosseinzadeh L, Gable RW. The non-templating synthesis of macro-cyclic Schiff base ligands containing pyrrole and homopiperazine and their binuclear nickel(II), cobalt(II) and mononuclear platinum(II) complexes: X-ray single crystal and anticancer studies. *J Mol Struct*. 2021;1244. doi: 10.1016/j.molstruc.2021.130956

36. Sangwan V, Singh DP. Template-engineered metal macrocyclic complexes: Synthesis and biological activity. *J Chinese Chem Soc*. 2020;67(6):1024-1031. doi: 10.1002/jccs.201900290

37. Rathi P, Singh DP. Investigation of divalent tetraazamacrocyclic complexes as potent antimicrobial and antioxidant agents. *Der Pharma Chem*. 2014;6(5):203-214.

38. Rathi P, Singh DP. Spectrochimica Acta Part A : Molecular and Biomolecular Spectroscopy Antimicrobial and antioxidant activity evaluation of Co (II), Ni (II), Cu (II). *Spectrochim Acta Part A Mol Biomol Spectrosc*. 2015;136:381-387. doi: 10.1016/j.saa.2014.09.044

39. S, Sharma V, Pradhan JK, Sharma SK, Singh P, Sharma JK. Structural, optical and antibacterial response of CaO nanoparticles synthesized via direct precipitation technique. *Nano Biomed Eng*. 2021;13(2):172-178. doi: 10.5101/NBE.V13I2.P172-178

40. Govindrajan M, Periandy S, Carthigayen K. FMO LUMO. *Spectrochim Acta - Part A Mol Biomol Spectrosc*. 2012;97:411-422.